European Journal of Cancer 151 (2021) 136–149

Available online at www.sciencedirect.com

ScienceDirect

journal homepage: www.ejcancer.com

Original Research

FGFR1 overexpression in non-small cell lung cancer is mediated by genetic and epigenetic mechanisms and is a determinant of FGFR1 inhibitor response

Olga Bogatyrova [a,1], Johanna S.M. Mattsson [b,1], Edith M. Ross [c,1], Michael P. Sanderson [a], Max Backman [b], Johan Botling [b], Hans Brunnström [d], Pinja Kurppa [b], Linnéa La Fleur [b], Carina Strell [b], Claudia Wilm [a], Astrid Zimmermann [a], Christina Esdar [a,2], Patrick Micke [b,*,2]

[a] *Translational Innovation Platform Oncology & Immuno-Oncology, Merck KGaA, Darmstadt, Germany*
[b] *Dept. of Immunology, Genetics and Pathology, Uppsala University, Uppsala, Sweden*
[c] *Translational Medicine, Merck KGaA, Darmstadt, Germany*
[d] *Division of Pathology, Lund University, Skåne University Hospital, Lund, Sweden*

Received 23 December 2020; received in revised form 11 March 2021; accepted 6 April 2021
Available online 10 May 2021

KEYWORDS
FGFR1;
Non-small cell lung cancer;
Promoter methylation;
miRNA;
Cancer immunity

Abstract Amplification of fibroblast growth factor receptor 1 (FGFR1) in non-small cell lung cancer (NSCLC) has been considered as an actionable drug target. However, pan-FGFR tyrosine kinase inhibitors did not demonstrate convincing clinical efficacy in *FGFR1*-amplified NSCLC patients. This study aimed to characterise the molecular context of FGFR1 expression and to define biomarkers predictive of FGFR1 inhibitor response.

In this study, 635 NSCLC samples were characterised for FGFR1 protein expression by immunohistochemistry and copy number gain (CNG) by in situ hybridisation (n = 298) or DNA microarray (n = 189). *FGFR1* gene expression (n = 369) and immune cell profiles (n = 309) were also examined. Furthermore, gene expression, methylation and microRNA data from The Cancer Genome Atlas (TCGA) were compared. A panel of *FGFR1*-amplified NSCLC patient-derived xenograft (PDX) models were tested for response to the selective FGFR1 antagonist M6123.

A minority of patients demonstrated *FGFR1* CNG (10.5%) or increased *FGFR1* mRNA (8.7%) and protein expression (4.4%). *FGFR1* CNG correlated weakly with FGFR1 gene and protein expression. Tumours overexpressing FGFR1 protein were typically devoid of

* *Corresponding author*: Dept. of Immunology, Genetics and Pathology, Uppsala University, 751 85 Uppsala, Sweden. Fax: +46 18 553354.
E-mail address: patrick.micke@igp.uu.se (P. Micke).
[1] These authors contributed equally to this work. [2] These authors contributed equally to this work.

https://doi.org/10.1016/j.ejca.2021.04.005

driver alterations (e.g. EGFR, KRAS) and showed reduced infiltration of T-lymphocytes and lower PD-L1 expression. Promoter methylation and microRNA were identified as regulators of FGFR1 expression in NSCLC and other cancers. Finally, NSCLC PDX models demonstrating *FGFR1* amplification and FGFR1 protein overexpression were sensitive to M6123.

The unique molecular and immune features of tumours with high FGFR1 expression provide a rationale to stratify patients in future clinical trials of FGFR1 pathway-targeting agents.

1. Introduction

The identification of activating mutations in the receptor tyrosine kinase (RTK) epidermal growth factor receptor (EGFR) in NSCLC patients and the subsequent approval of EGFR inhibitors, such as gefitinib and erlotinib, heralded a new era of targeted therapy in the treatment paradigm of NSCLC [1,2]. This initial breakthrough was followed by the approval of other targeted therapies in molecularly defined NSCLC patients, such as those harbouring ALK or ROS1 fusions and more recently, the development of more effective second- and third-generation agents, which selectively target the mutant forms of oncogenic driver proteins like EGFR and ALK [3,4].

These findings raised the tantalising possibility that additional oncogenic driver alterations could be identified to guide the application of novel targeted agents [5]. Indeed, in-depth characterisation of the genomic landscape of lung cancer has identified aberrations in the RTKs *BRAF, RET*, *MET, NTRK1/2/3* and *ERBB2* [4,6,7]. While initial clinical trials of non-selective TKIs demonstrated disappointing activity in NSCLC patients harbouring such alterations, potentially as a result of the adverse safety profiles of these agents precluding adequate target inhibition [8–10], more recent trials of highly selective MET, RET or TRK inhibitors yielded response rates between 50 and 80% [11,12], confirming the driver status of these alterations and justifying the approval of these drugs. These successes have led to the more recent development of novel targeted agents against underserviced driver alterations, including those previously considered undruggable, such as the G12C mutated form of KRAS [13,14].

Fibroblast growth factor receptor 1 (FGFR1) has long been proposed as a promising target in squamous cell carcinoma of the lung. The FGFR family comprises four isoforms (FGFR1-4), which bind specific FGF ligands, of which there are 22 different members. Ligand engagement induces FGFR dimerisation and activation of the canonical mitogen-activated protein kinase (MAPK) and phosphoinositide 3-kinase (PI3K) pathways to promote diverse cellular fates including proliferation, differentiation and survival. Genomic alterations of FGF-pathway genes have been identified in several cancer types, including those of the bladder, endometrial gland, lung, breast and intrahepatic cholangiocarcinoma [15–17]. This knowledge led to the successful clinical development and approval of FGFR TKIs in urothelial carcinoma patients harbouring *FGFR3* or *FGFR2* alterations [18] and cholangiocarcinoma patients with *FGFR2* fusions or rearrangements [19].

In the case of FGFR1, a pivotal study from Weiss *et al.* [20] revealed the presence of *FGFR1* amplification in 22% of lung squamous cell carcinoma patients. These authors also demonstrated that the proliferation and survival of *FGFR1*-amplified NSCLC cell lines were reduced by treatment with the FGFR TKI PD173074. Furthermore, *FGFR1* amplification may represent an oncogenic driver and mediator of drug resistance in other malignancies such as breast cancer [21].

Despite these promising findings, early clinical trials of FGFR TKIs in *FGFR1*-amplified NSCLC patients yielded only moderate response outcomes [22–25]. This contrasted to the strong responses of patients with FGFR2- or FGFR3-altered cancers to FGFR TKIs [18,19]. These clinical findings highlight the importance of further analysis of the tumourigenic role of FGFR1 alterations, the optimal pharmacological approach for FGF-pathway inhibition and the identification of predictive biomarkers beyond *FGFR1* CN in order to guide future trials. The aims of this study were to comprehensively evaluate the role of FGFR1 expression in the genomic background of human NSCLC and other cancers and to redefine patient groups that may benefit from selective FGFR1 inhibition.

2. Materials and methods

2.1. Patient cohorts

The patient population consisted of 661 operated NSCLC patients based on two patient cohorts. Only patients with adenocarcinoma, squamous cell carcinoma and large cell histology were included. The first cohort (Uppsala 1) consisted of 349 patients surgically resected between 1995 and 2005 at the Uppsala University

Hospital. The second cohort (Uppsala 2) included 312 patients resected between 2006 and 2010 at the Uppsala University Hospital. The characteristics of each patient cohort are summarised in Supplemental Table S1.

The analysis of human tissue specimens and corresponding clinicopathological data was approved by the Uppsala Regional Ethical Review Board (#2006/325 and #2012/532) and performed in accordance with the Swedish biobank legislation.

A validation data set of two lung cancer cohorts (lung adenocarcinoma and lung squamous cell carcinoma) with 1103 samples (tumours, n = 1003; normal tissue, n = 110) was extracted from The Cancer Genome Atlas (TCGA). The characteristics of each cohort are described in Supplemental Table S2.

Additional data sets from 14 TCGA cancer cohorts (BLCA, BRCA, CHOL, COAD, ESCA, HNSC, KIRC, KIRP, LIHC, PAAD, PRAD, READ, THCA and UCEC) with 6297 samples (tumours, n = 5757; normal tissue, n = 540) were extracted from TCGA. Only primary tumour samples and adjacent normal tissue samples were used for analysis.

2.2. Tissue microarray (TMA) generation

TMAs were generated as described previously from formalin-fixed, paraffin-embedded (FFPE) samples from Uppsala 1 [26,27] and Uppsala 2 [28,29]. Briefly, all specimens were reviewed by pathologists (HB, PM and JB) and representative areas were encircled on tissue slides before cores were taken from corresponding tissue blocks and incorporated into recipient blocks. All tumour samples were included in duplicates (2 × 1 mm tissue cores).

2.3. Immunohistochemistry (IHC)

For the IHC staining of FGFR1, sections of 4 μm from the TMAs and from FFPE patient-derived xenograft (PDX) tumour samples were mounted on charged slides (SuperFrost Ultra Plus, Thermo Fisher Scientific). The staining procedure was performed using a Discovery® XT (Roche Diagnostics) instrument. Following deparaffinisation, the sections were heated for epitope retrieval in Tris-EDTA buffer of pH 8. The sections were then incubated with the primary monoclonal antibody against FGFR1 (clone EPR806Y, Abcam) diluted to 20 μg/ml in phosphate-buffered saline (PBS) or the isotype control antibody (clone DA1E, rabbit monoclonal IgG, New England Biolabs) followed by the corresponding detection kits (Discovery® XT). Slides were counterstained with haematoxylin, washed in tap water, dehydrated and mounted on glass slides in Entellan® Neu (VWR International) permanent mounting media.

The TMA slides were scanned using an Aperio ScanScope XT (Aperio Technologies Inc.) whole slide scanner to generate high-resolution digital images. The scanned images were then viewed in 20× magnification using ImageScope (Aperio Technologies Inc.). FGFR1 protein expression was annotated semi-quantitatively, and the staining intensity was categorised based on a four-graded scale: negative (0), weak (1), moderate (2) and strong (3). The fraction of stained tumour cells was evaluated based on a nine-graded scale: 0–1% (1), 2–5% (2), 6–10% (3), 11–20% (4), 21–30% (5), 31–40% (6), 41–50% (7), 51–75% (8) and >75% (9). Samples were classified as positive when at least 2% of the tumour cells displayed moderate or strong staining (fraction of positive cells ≥ 2, intensity ≥ 2).

IHC-stained PDX tumour sections were scanned using an AxioScan (Zeiss) instrument with a resolution of x/y: 1 pixel = 0.44 × 0.44 μm^2. The scans were analysed with the image analysis software VIS (Visiopharm). To determine the amount of antigen present, the percentage of positive/brown-stained area was calculated relative to the total area of viable tissue: 100 × [brown area/(brown area + blue area)]. Here, the brown area represented positive immune staining and the blue area indicated the haematoxylin-stained cell nuclei and cytoplasm. VIS was used to measure the intensity of the brown colour on a scale of 0 (=black) to 255 (=white). Antibody staining was calculated as arbitrary units (AU) based on the formula: positive area (%) × (255 − intensity)/100.

The IHC staining of immune markers was performed as previously described [30,31]. A detailed description of the immune marker staining protocol and the definition of cut-offs can be found in the Supplemental Methods.

2.4. Molecular analyses of Uppsala cohorts 1 and 2

The staining of the fluorescent in situ hybridisation (FISH) slides was performed on the Uppsala 2 cohort according to the manufactures' instructions (ZytoVision). The categorisation of *FGFR1* amplification status was performed in accordance with that described previously by Schildhaus [32].

RNA from frozen tumour tissue from 193 patient samples from the Uppsala 1 cohort was used for gene expression microarray analysis, as previously described [27]. Four quantiles (25%, 50%, 75% and 90%) of the distribution of *FGFR1* gene expression values were defined to categorise samples as displaying either very high, high, middle or low expression.

DNA from frozen tumour tissue from 189 patient samples from the Uppsala 1 cohort was used for single-nucleotide polymorphism (SNP) analysis of gene CN variations (GSE76730), as previously described [33]. Samples were categorised into three groups based on *FGFR1* CN status: high amplification (CN > 3), amplification (CN ≥ 2.5 and ≤3) and no event (CN < 2.5).

RNA from frozen tumour tissue from 185 patient samples from the Uppsala 2 cohort was used for RNA sequencing (RNAseq), as previously described [34]. Four quantiles (25%, 50%, 75% and 90%) were set to categorise samples based on *FGFR1* gene expression into either of the following groups: very high, high, middle and low expression. Samples were further categorised into high- or low-FGFR1 expression groups using an outlier sum statistic method [35].

For targeted deep sequencing of 82 lung cancer-related genes from 321 patient samples from the Uppsala 2 cohort, target enrichment was performed using the Haloplex system (Agilent Technologies, Santa Clara, CA) as previously described [36]. Sequencing was done with the Illumina HiSeq 2500 platform (Illumina, San Diego, CA).

Detailed descriptions of the protocols for FISH, gene expression microarrays, SNP arrays, RNAseq and mutational analyses can be found in the Supplemental Methods.

2.5. Statistical analysis of Uppsala 1 and 2 cohorts

Correlation analyses of different data readouts were performed using the Spearman correlation method (cor function in the ggpubr R package). For survival analysis, Cox proportional hazard models using different data sources were fitted using the survival R package. Age, stage and performance status were included as covariates in the model. Survival curves were plotted, using the ggsurvplot function of the survminer R package. The p-values were adjusted using the Benjamini & Hochberg adjustment method (stats R package) for the multiple comparisons. Mutual exclusivity between FGFR1 expression and immune markers was evaluated using a one-sided Boschloo's exact test (exact.test function in Exact R package using 'boschloo' as the method and 'less' as the alternative).

2.6. Analysis of data from TCGA

Gene expression data were downloaded from the recount2 data portal [37]. The methylation, gene mutation and miRNA data for selected TCGA cancer cohorts were downloaded from the GDC data portal (https://gdc.cancer.gov). The extraction dates were as follows: mRNA on 10/2018, methylation and miRNA on 10/2017 and gene CN and mutations on 6/2019. *FGFR1* promoter methylation was assessed using the average value of 3 CpGs (cg10823844, cg15791248 and cg27646230). The expression of selected genes was evaluated using transcript per million (TPM) values, and this was used to define groups based on differential expression using the outlier sum statistic method [35]. Patients were only included when gene expression or methylation data were available. Correlations between the expression of FGFR1 mRNA and different miRNAs were calculated using the Spearman method (cor function in the ggpubr R package). The Bonferroni–Hochberg method was used for multiple testing correction.

For survival analyses, a Cox proportional hazard model was fitted, taking age and stage into account as covariates (survival R package). Survival curves were plotted using the ggsurvplot function from the survminer R package. For the oncoprint visualisation, common driver alterations were summarised as described above. Patients were only included if at least gene expression, gene CN and mutation data were available (492 and 464 patients for lung adenocarcinoma and lung squamous cell carcinoma, respectively). Exon skipping for specific genes was evaluated based on alternative splicing data generated by Kahles *et al.* [38]. Samples were defined as positive for *MET* exon 14 skipping when they displayed a Percent Spliced In Value < 0.5. *NFE2L2* exon skipping positivity was defined based on a Percent Spliced In Value < 0.9. Samples were categorised into groups based on the degree of PD-L1 expression (TPM) and tumour mutational burden (non-silent nucleotide variants per megabase pair) [39] by applying a previously described outlier sum statistical method [35].

2.7. PDX models

The sources of the PDX models as well as the animal ethics compliance measures are detailed in the Supplemental Methods. For each PDX model, tumour fragments were implanted into the flanks of female immunocompromised nude (Athymic Nude-Foxn1nu; NMRI-Foxn1nu; Crl:Nu(NCr)-Foxn1nu) or NOD-SCID (NOD.CB-17-Prkdcscid/NCrHsd) mice. Each PDX model included two experimental groups, which were treated twice weekly intraperitoneally with either vehicle or M6123 at a dose of 12 mg/kg. PDX experiments using models annotated with the prefix ST and LU consistent with one mouse per experimental groups, while the CTG0924 and LXFL1121 experiments used ten mice per group. The end-point of each study was defined by the tumour volume (TV) of the vehicle-treated control group. To account for growth rate variations between the different models, studies were terminated and end-points (Relative TV $[TV_{\text{treatment start}} - TV_{\text{treatment end}}]/[TV_{\text{treatment start}}]$) were calculated when the control TV reached 1000 mm^3. Tumour models exhibiting relative TV change values $\leq 73\%$ were categorised as responders to M6123. This cut-off was selected in accordance with the Response Evaluation Criteria In Solid Tumours (RECIST) definition for progressive disease for the volume of solid tumours and corresponds to the 20% cut-off parameter for the longest tumour diameter [40].

3. Results

3.1. FGFR1 protein and gene expression and gene copy number in NSCLC patients

The expression of FGFR1 protein in 661 patient samples from the Uppsala 1 and 2 cohorts was examined by IHC using a rabbit monoclonal antibody (Fig. 1A). The selectivity of this antibody for FGFR1 over other FGFR isoforms was confirmed using a panel of human cell lines selected based on the amplification of FGFR family members (Supplemental Fig. S1; Supplemental Table S3). Positive staining, characterised by predominantly diffuse cytoplasmic and/or membrane localisation (Fig. 1A), was observed in 26 of 635 evaluable cases (4.4%) on the complete NSCLC cohort, 3.5% in the adenocarcinoma and 6.0% in the squamous cell carcinoma subgroups. Normal lung tissue, including alveolar and bronchial epithelial cells, did not display significant FGFR1 protein expression.

In order to compare protein expression with gene CN, FISH analysis was performed on the Uppsala 2 cohort (n = 298). Furthermore, gene CN values were calculated from SNP array data from 189 patients on the Uppsala 1 cohort. These data were complemented with gene expression data based on microarrays from the Uppsala 1 cohort and RNAseq data from the Uppsala 2 cohort (Fig. 1B and C). A poor correlation between *FGFR1* gene CN and FGFR1 gene and protein expression was observed (rho = (0.06–0.33)). In contrast, a stronger correlation was detected between FGFR1 mRNA and protein expression (rho = (0.18–0.5)) (Fig. 1D). The protein–mRNA correlation was comparable to that previously described for other markers in lung cancer [31]. Together, these findings suggest that mechanisms beyond gene amplification contribute to the overexpression of FGFR1 in a subset of NSCLC patients.

3.2. Profiling of the landscape of oncogenic driver alterations in FGFR1-protein overexpressing NSCLC patients

FGFR1 IHC expression was compared to the gene alteration events that are commonly found in NSCLC using the Uppsala 2 cohort (n = 312) [36] (Fig. 2A, Supplemental Table S4). Two adenocarcinoma cases exhibiting FGFR1 overexpression (FGFR1^{high}) harboured mutated EGFR. No other oncogenic mutations in *KRAS*, *BRAF*, *MET* or *PIK3CA* were detected in FGFR1^{high} adenocarcinoma patients (n = 7). Only two concurrent *KEAP1* mutations were identified in FGFR1^{high} lung squamous cell carcinoma patients (n = 7). These findings suggest that the FGFR1 overexpression in NSCLC defines a distinct molecular subgroup lacking other known oncogenic driver alterations.

3.3. FGFR1 protein expression and the immune microenvironment of NSCLC

We next compared the in situ expression of diverse immune markers and FGFR1 protein on the Uppsala 2 cohort. A trend of mutual exclusivity between FGFR1 protein expression and the presence of immune markers and cells in the tumour and stromal compartment was observed (Fig. 2B; Supplemental Fig. S2; Supplemental Table S5). A significant inverse relationship was detected between FGFR1 protein expression and the infiltration of CD3+ and CD8 lymphocytes in tumour tissue (stromal and tumour compartments, CD3: $p = 0.02$, CD8: $p = 0.03$). PD-L1 protein expression in the tumour compartment also showed mutual exclusivity with FGFR1 protein overexpression ($p = 0.02$). Taken together, these findings suggest that FGFR1^{high} NSCLC tumours exhibit features indicative of reduced immune infiltration and activation.

3.4. FGFR1 expression and patient outcome

For survival analysis, patients were stratified according to dichotomised *FGFR1* gene CN, FGFR1 gene and protein expression, and histological subtypes using the Uppsala 1 and 2 data sets. Elevated tumour FGFR1 mRNA expression was associated with longer overall survival in squamous cell carcinoma patients ($p = 0.007$; Fig. 2C). No other significant associations were detected, albeit a weak trend ($p = 0.19$) towards longer survival was observed in lung squamous cell carcinoma patients with high FGFR1 protein expression (Supplemental Fig. S3).

3.5. FGFR1 expression on TCGA lung cancer patient cohorts

NSCLC patient data from TCGA were used as an independent cohort to confirm the findings on the Uppsala cohorts described above. Molecular information was extracted including mutational status, gene CN, mRNA and miRNA expression and methylation data. Consistent with the findings on the Uppsala cohorts, FGFR1 mRNA overexpression did not commonly co-occur with known driver alterations in lung adenocarcinoma (FGFR1^{high} frequency = 9.8%) and lung squamous cell carcinoma case (FGFR1^{high} frequency = 14.4%) samples from TCGA (Fig. 3). Similar to the findings on the Uppsala cohorts described above, a trend towards improved survival probability

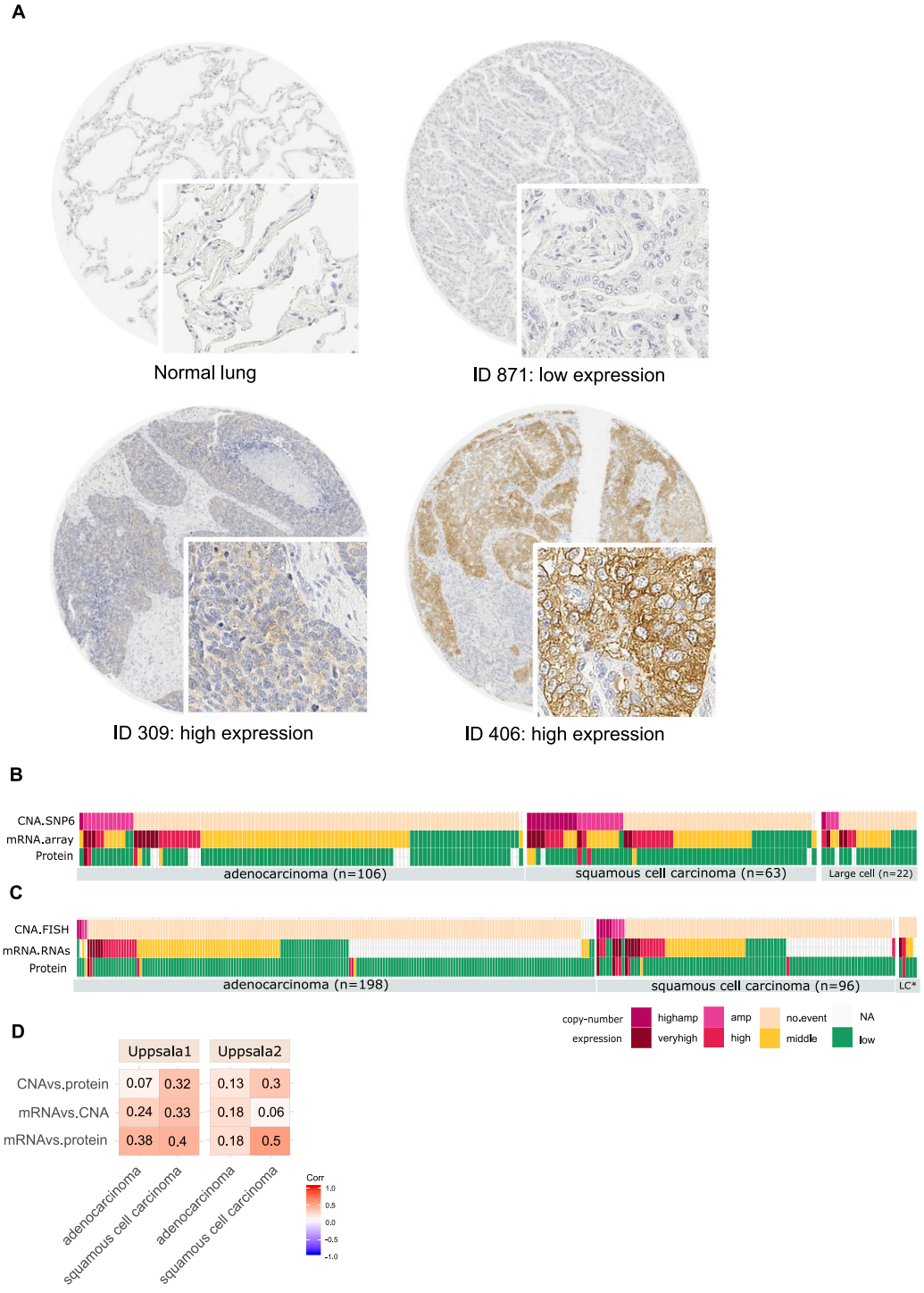

Fig. 1. Correlation of FGFR1 protein, mRNA and CN. (*A*) Immunohistochemical (IHC) staining was performed on a TMA with the monoclonal FGFR1 antibody (clone EPR806Y). Manual annotation of both the staining intensity and the fraction of stained cells was performed. High FGFR1 expression in samples was defined by either moderate or strong staining in ≥2% of the tumour cells, remaining samples were classified as having low FGFR1 expression. The oncoprints indicate *FGFR1* CN and FGFR1 mRNA and protein expression for samples on the Uppsala 1 (*B*) and Uppsala 2 (*C*) cohorts. (*D*). The indicated heatmaps show correlation matrices for FGFR1 protein and mRNA expression and *FGFR1* CN for patients on the Uppsala 1 and Uppsala 2 cohorts. The heatmaps represent rho correlation coefficients with the degree of red intensity indicating an increasingly positive correlation.

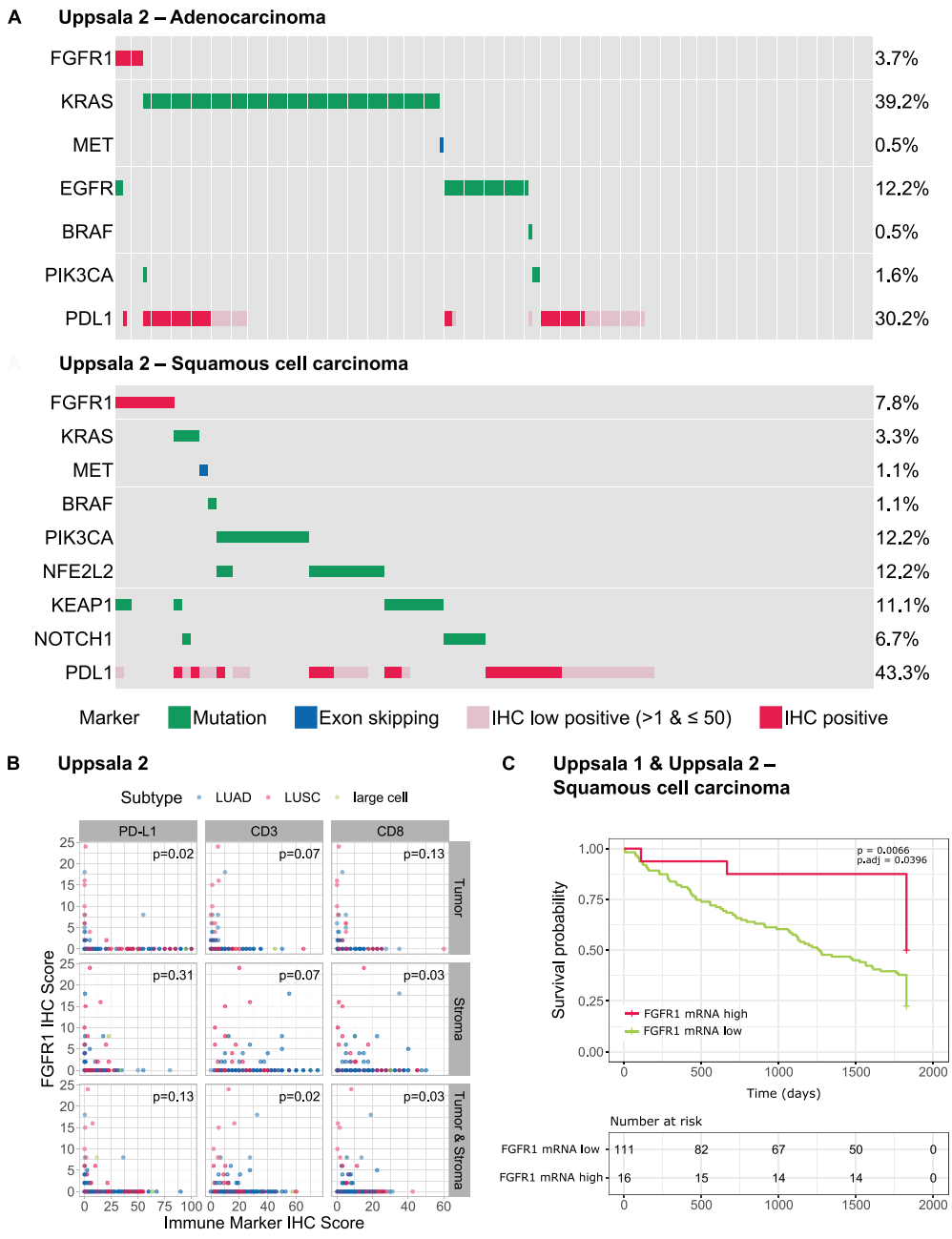

Fig. 2. Association of FGFR1 expression with mutation status, immune markers and survival. (*A*) The oncoprints indicate the FGFR1 IHC status, the presence of mutations in oncogenic driver genes and the PD-L1 protein expression from samples of the Uppsala 2 cohort. Adenocarcinoma and squamous cell carcinoma samples are depicted separately. (*B*) Scatterplots of FGFR1 IHC scores and the indicated immune marker IHC scores from samples of the Uppsala 2 cohort are indicated. P-values were assessed using a one-sided Boschloo's exact test on dichotomised values. The histological subtypes are distinguished by colour (LUAD: lung adenocarcinoma, LUSC: lung squamous cell carcinoma). (*C*) Kaplan–Meier curves of the probability of survival for patients stratified by FGFR1 mRNA expression status for squamous cell carcinoma patients combined from the Uppsala 1 and Uppsala 2 cohorts are indicated.

was observed in FGFR1^{high} patients on the TCGA lung squamous cell carcinoma cohort (Supplemental Fig. S4).

3.6. DNA methylation and miRNAs regulate FGFR1 expression in NSCLC and other tumour entities

As *FGFR1* CN did not show a strong relationship to FGFR1 overexpression, we next examined the involvement of epigenetic regulatory mechanisms including DNA methylation and miRNAs. The DNA methylation status of *FGFR1* was examined in 824 lung adenocarcinoma and squamous cell carcinoma patients from TCGA. A significant negative correlation for both NSCLC subtypes (p(LUAD) $<$ 0.001, p(LUSC) $<$ 0.001) was observed between FGFR1 mRNA expression and the methylation of three CpGs

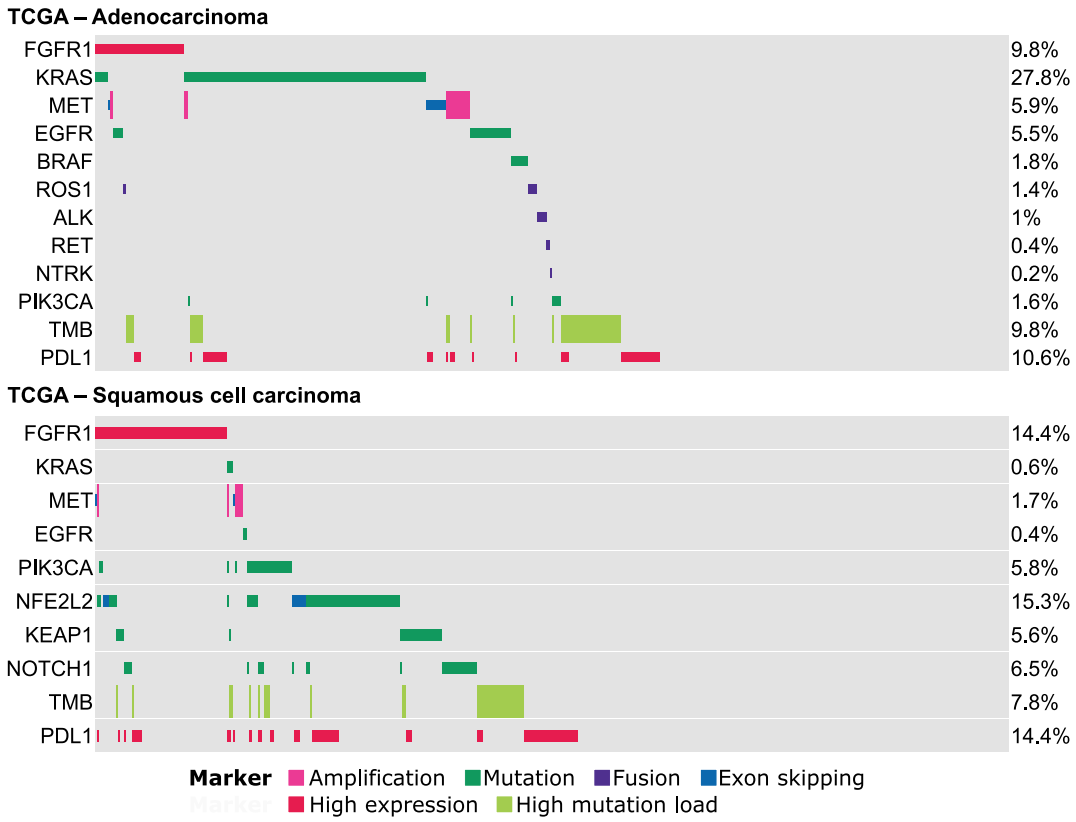

Fig. 3. Comparison of FGFR1 mRNA expression with the mutational status of oncogenic driver genes. The oncoprints indicate FGFR1 mRNA expression status, mutational status of known oncogenic driver genes, estimated tumour mutational burden (TMB) and PD-L1 mRNA expression from 492 to 464 patients from TCGA cohorts for lung adenocarcinoma and squamous cell carcinoma, respectively.

(cg10823844, cg15791248 and cg27646230) located in the *FGFR1* promoter (Fig. 4A).

We next expanded our correlation of methylation and FGFR1 expression to 14 other solid tumour data sets from TCGA. As in NSCLC, a subset of cases from several cancer types demonstrated *FGFR1* promoter hypomethylation, which was associated with elevated FGFR1 mRNA expression (Fig. 4B). This was particularly evident in breast, head and neck, oesophageal, bladder and endometrial cancers. This suggests that hypomethylation of specific *FGFR1* promoter sites may represent a shared mechanism underpinning FGFR1 overexpression across diverse cancer types.

We next used NSCLC patient data from TCGA to examine the role of miRNAs in the control of FGFR1 expression. Our initial analysis included 58 miRNAs extracted from the miRTarBase database (Release 7.0) (Supplemental Table S6), which have previously been experimentally validated for their effect on FGFR1 expression by employing miRNA knockdown or overexpression approaches in conjunction with reporter assays, western blotting or microarray analyses [41]. The selected miRNAs were found to either positively or negatively associate with FGFR1 mRNA expression (Fig. 5A). The most significant negative correlation on both the adenocarcinoma and squamous cell carcinoma patient subsets was observed for Hsa-mir-16-1. We next extended our correlation analysis to other tumour types that demonstrated a broad distribution of FGFR1 mRNA expression including breast, head and neck, oesophageal, bladder and endometrial cancers. The expression of eight different miRNAs negatively correlated with FGFR1 mRNA levels in these cancer types (Fig. 5B). Taken together, these results suggest that deregulation of specific miRNAs may lead to FGFR1 overexpression in NSCLC and other cancers.

3.7. Targeting FGFR1 in patient-derived xenograft models of lung cancer

FGFR1 amplification has previously been applied for patient enrolment in clinical trials of FGFR TKIs [24,25]. Therefore, we screened a large panel of NSCLC PDX models (n = 96) for *FGFR1* amplification by FISH and identified ten (10.4%) positive cases based on the criteria previously defined by Schildhaus *et al.* [32]. These ten tumour models were assessed for response to the selective monovalent FGFR1 antagonist M6123 [42,43]. Inhibition of tumour growth following M6123 treatment was observed in two of the PDX models, while the other eight models did not respond. IHC analysis of treatment naïve PDX tumour material

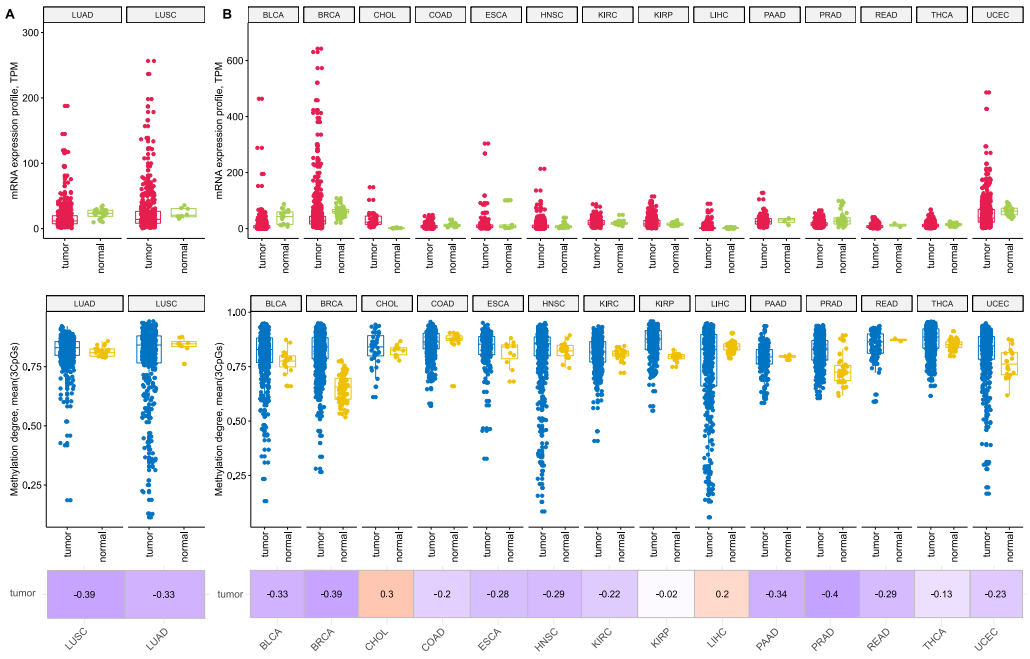

Fig. 4. FGFR1 mRNA expression and promoter methylation in TCGA cohorts. (*A*) The differences in FGFR1 mRNA expression profiles in tumours and normal tissue samples in lung cohorts (TCGA-LUAD, TCGA-LUSC) are represented as dot plots (upper plot, red denotes tumour and light green indicates normal tissue). FGFR1 mRNA expression was correlated with the DNA methylation status for the *FGFR1* promoter (lower plot, blue denotes tumour and yellow indicates normal tissue). The correlation between FGFR1 mRNA and methylation (average of 3 CpGs sites: cg10823844, cg15791248 and cg27646230) in tumour samples is shown as a heatmap of rho correlation coefficients (blue denotes high negative correlation and red indicates a high positive correlation). (*B*) The same analyses described in *A* were performed for the indicated tumour types. Abbreviations: BLCA: Urothelial Bladder Carcinoma, BRCA: Breast Invasive Carcinoma, CHOL: Cholangiocarcinoma, COAD: Colon Adenocarcinoma, ESCA: Oesophageal Carcinoma, HNSC: Head-Neck Squamous Cell Carcinoma, KIRC: Kidney Renal Clear Cell Carcinoma, KIRP: Kidney Renal Papillary Cell Carcinoma, LIHC: Liver Hepatocellular Carcinoma, PAAD: Pancreatic Adenocarcinoma, PRAD: Prostate Adenocarcinoma, READ: Rectum Adenocarcinoma, THCA: Thyroid Cancer, UCEC: Uterine Corpus Endometrial Carcinoma.

revealed the highest FGFR1 expression in the two M6123 responders (Fig. 6; Supplemental Table S7). These data suggest that FGFR1 protein expression may represent an important determinant of response to agents targeting the FGF pathway.

4. Discussion

This study defined a subgroup of lung cancer patients exhibiting overexpression of FGFR1 mRNA and protein. FGFR1 overexpression was only weakly linked to *FGFR1* amplification and could better be explained by promoter demethylation or downregulation of specific miRNAs. Tumours with high FGFR1 expression usually lacked other oncogenic driver mutations (e.g. EGFR or KRAS) and also showed a distinct immune desert tumour microenvironment phenotype. Selective targeting of FGFR1 in *FGFR1*-amplified PDX models delivered activity in tumours with high FGFR1 protein expression. Taken together, this study provides a strong rationale to re-evaluate FGFR1 inhibitors in NSCLC and suggests that immunohistochemical analysis of FGFR1 protein levels could be an appropriate approach for patient selection.

Initial interest in FGFR1 as a therapeutic target in squamous cell carcinoma of the lung was based on the study of Weiss *et al.* [20], in which 155 primary squamous cell lung carcinoma samples were evaluated by SNP microarrays. Fifteen of 155 cases (9.7%) demonstrated *FGFR1* amplification (CN $\geq$ 4) based on the GISTIC algorithm. In an independent squamous cell lung carcinoma cohort, 22% of patients showed high-level *FGFR1* amplification (CN $>$ 9) using a specific FISH probe. Furthermore, these authors demonstrated that selected *FGFR1*-amplified NSCLC cell lines were sensitive both *in vitro* and *in vivo* to the FGFR TKI PD173074. In a subsequent study, the FGFR TKI AZD4547 was shown to only deliver efficacy in *FGFR1*-amplified lung cancer cell lines and PDX models [44]. These promising preclinical data supported the initiation of several clinical trials of FGFR TKIs in patients with lung squamous cell carcinoma and *FGFR1* amplification. In a phase I trial of AZD4547 in 15 patients exhibiting *FGFR1* amplification, only one objective

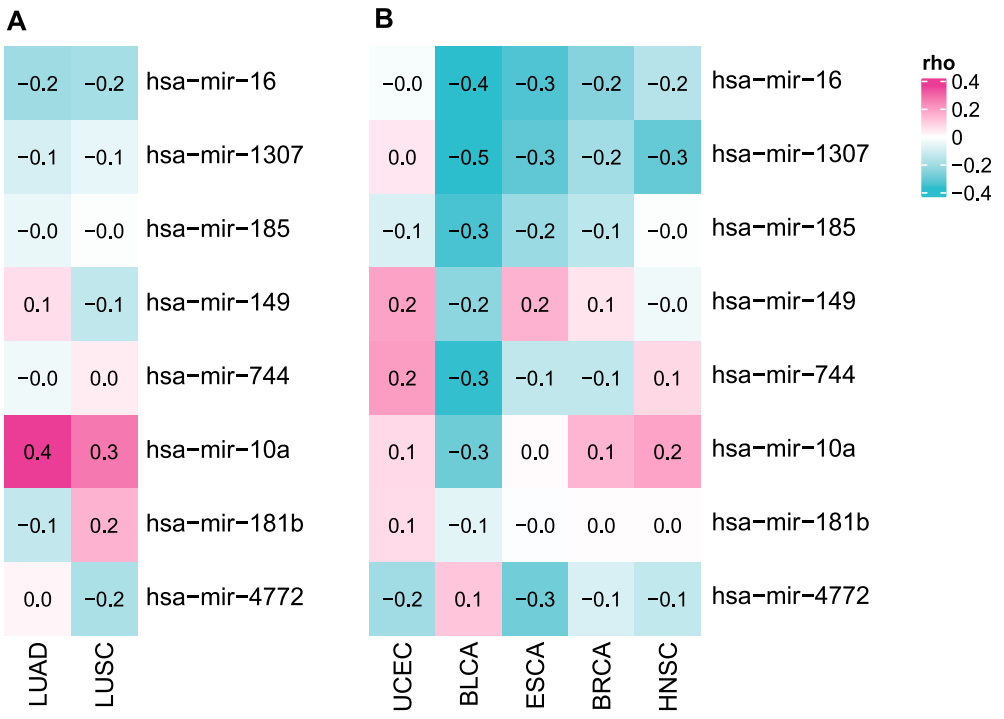

Fig. 5. Correlation of miRNAs with FGFR1 expression on TCGA cohorts. The heatmap depicts miRNA negatively correlating with FGFR1 mRNA expression in lung cancer (*A*) and other cancer types as indicated (*B*). The heatmap represents rho correlation coefficients with blue and red indicating an increasing negative or positive correlation, respectively. Abbreviations: BLCA: Urothelial Bladder Carcinoma, BRCA: Breast Invasive Carcinoma, ESCA: Oesophageal Carcinoma, HNSC: Head-Neck Squamous Cell Carcinoma, LUAD: Lung Adenocarcinoma, LUSC: Lung Squamous Cell Carcinoma, UCEC: Uterine Corpus Endometrial Carcinoma.

response was observed [25]. In a sub-study of the Lung-MAP trial, AZD4547 delivered responses in only 2 of 27 (7%) of NSCLC patients exhibiting *FGFR1* amplification [22]. Another FGFR TKI infigratinib (BGJ398) was assessed in a phase I trial, in which 4 of 36 (11%) *FGFR1*-amplified patients developed a partial response [24].

This reported activity of FGFR TKIs in *FGFR1*-amplified patients was lower than expected for a precision therapy target. Furthermore, since these inhibitors are not selective for FGFR1, their effects could potentially be mediated via FGFR2 and/or FGFR3 inhibition [45]. Consequently, the value of *FGFR1* amplification as a biomarker to select NSCLC patients for FGFR inhibitor treatment has recently undergone critical reassessment [17]. Indeed, a preclinical study suggested that lung cancer cell lines with high FGFR mRNA or protein expression were sensitive to the multi-kinase inhibitor ponatinib, which has activity against the FGFR family [46]. Similarly, Kotani *et al.* [47] demonstrated that only lung cancer cell lines with *FGFR1* amplification and high FGFR1 protein expression were sensitive to a panel of FGFR inhibitors. Another study using PDX models of lung squamous cell carcinoma suggested that FGFR1 mRNA expression strongly predicts response to infigratinib [48]. Recently, a large phase 1 study of the pan-FGFR inhibitor rogaratinib demonstrated efficacy in urothelial cancer patients positive for FGFR3 mRNA expression [49]. These published findings are in line with our observation in PDX models that *FGFR1* amplification is not sufficient to predict response to FGFR1-directed therapy and that high protein expression might be a better predictive biomarker.

So far, only a few reports have evaluated the correlation of *FGFR1* amplification with FGFR1 expression in larger NSCLC patient cohorts. While one study indicated a significant correlation between *FGFR1* CN and protein expression in the squamous cell carcinoma subgroup [50], another report found no association between FGFR1 immunostaining and gene amplification in a cohort of 265 NSCLC cases [51]. A more recent study of 90 squamous NSCLC samples showed that while *FGFR1* amplification was associated with significantly higher FGFR1 expression, many non-amplified samples also demonstrated elevated FGFR1 levels [52]. In keeping with our findings, these researchers also described a stronger correlation between FGFR1 mRNA and protein expression, compared to that between *FGFR1* amplification and FGFR1 expression [52]. The discrepancies between these studies may be due to the use of alternate methodologies and cut-offs for the assessment of *FGFR1* amplification and FGFR1 mRNA and protein overexpression. We performed thorough validation of the sensitivity and specificity of our FGFR1 immunostaining protocol and employed the widely accepted Schildhaus criteria for the definition of

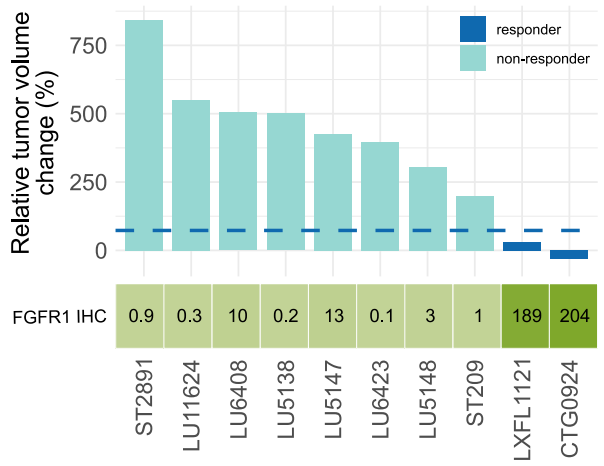

Fig. 6. Antitumour efficacy of the selective FGFR1 antagonist M6123 in *FGFR1*-amplified lung cancer PDX models with differential FGFR1 protein expression levels. All lung cancer PDX models tested were positive for *FGFR1* amplification, as assessed by FISH. The waterfall plot indicates the antitumour response of each PDX model to the FGFR1 antagonist M6123. Models showing a relative tumour volume change below 73% (dashed horizontal line) were classified as responders, as described in the Materials and Methods section. The response status of each model to M6123 is indicated (dark blue = responder, light blue = non-responder). The heatmap indicates the intensity of FGFR1 expression, as determined by IHC. The histological subtype of each PDX model as well as FGFR1 IHC staining and relative tumour volume data is shown in Supplemental Table S7.

FGFR1 amplification [32]. Applying these methods, it could be clearly demonstrated that high FGFR1 expression cannot be solely explained by *FGFR1* amplification and as such, we examined the role of other regulatory mechanisms.

Our analysis of TCGA data sets suggested that promoter hypomethylation activates FGFR1 expression in a subset of lung cancer cases. Interestingly, this was also observed in several other cancer types, including breast and prostate cancer, indicating a general relevance of this epigenetic mechanism independent of the cancer type. We furthermore identified a group of miRNAs that negatively correlated with FGFR1 mRNA expression. Several of these have been previously established as FGFR1 targets, while others have not been linked to FGFR1. Deregulation of Hsa-miR-16-1 has been described in diverse tumour types including lung and breast cancers and haematologic malignancies [53]. Here, we show that Hsa-miR-16-1 is associated with FGFR1 expression in both main lung cancer histologies and in four other cancer types. Interestingly, miRNA Hsa-miR-16-1 was previously described to be decreased in lung fibroblasts from smokers [54]. In the same study, a lung cancer co-culture model was used to demonstrate that miRNA Hsa-miR-16-1 regulates the tumourigenic function of fibroblasts, partly via modulation of FGFR1 expression. Taken together, these findings suggest the existence of two previously undescribed mechanisms that underpin FGFR1 overexpression in diverse cancers. Other regulative mechanisms might also be involved as previously demonstrated in the study of Lu *et al.* [55], who showed that the Hippo/YAP1 pathway regulates FGFR1 expression on a transcriptional level and modulates cancer stem-like cell properties of *FGFR1*-amplified lung cancer cells *in vitro* and *in vivo*.

Several key findings based on our unique patient cohorts indicate that FGFR1 overexpression defines a distinct subset of lung cancer with unique molecular, immune and prognostic features. Firstly, we noted that lung cancers with elevated tumour FGFR1 expression commonly lack other known driver alterations.

Furthermore, we found that FGFR1 overexpression is associated with improved prognosis in squamous lung carcinoma. It should be noted that previous reports have only evaluated the prognostic impact of *FGFR1* amplification or FGFR1 protein expression and have mostly described an association of these markers with poorer patient outcome [56]. To our knowledge, our study is the first to examine the prognostic impact of FGFR1 mRNA expression. Our analyses identified a strong positive correlation between FGFR1 mRNA and patient survival in the Uppsala cohorts and a non-significant ($p = 0.16$) trend in the lung squamous cell cancer cohort from TCGA. The improved survival associated with FGFR1 mRNA overexpressing, despite a relatively low infiltration of immune cells, is analogous to previous reports on the immune landscape and prognostic impact of EGFR alterations in lung cancer [57–59]. Future studies are warranted to investigate the underlying mechanism by which FGFR1 influences patient outcome, such as tumour aggressiveness, therapy response and drug resistance.

We demonstrate for the first time that elevated FGFR1 expression in lung cancers is associated with reduced tumour immunity. This included decreased tumour infiltration of lymphocytes and other immune cell markers. Previous reports have suggested that tumour intrinsic oncogenic signalling pathways play important roles in modulating the immune microenvironment. For instance, STK11 (alias LKB1) mutation in human tumours is associated with reduced CD8+ lymphocyte infiltration and PD-L1 expression [60]. Meanwhile, *in vivo* STK11 knockout led to the recruitment of immune suppressive cells in the tumour microenvironment [61]. Aberrations in the WNT/β-catenin pathway have also been described to associate with a 'non-inflamed' signature in diverse solid tumour types [62], while experimental tumour models harbouring activated β-catenin exhibited impaired T-cell priming and recruitment [63]. Finally, lung cancer tissue with activating EGFR mutations revealed a desert immune phenotype characterised by reduced infiltration of macrophages and T-cells and lower PD-L1 expression [64]. Of note, EGFR inhibition has been shown to

improve the efficacy of PD-L1 inhibitors in experimental cancer models [65]. Our analogous findings in FGFR1-overexpressing lung cancers provide a basis for future experimental analysis of the combinatorial effects of FGFR1 inhibitors with immune therapies, as a first step towards the potential clinical realisation of this novel therapeutic strategy.

Our characterisation of the molecular status of the FGFR1 in lung cancer is based on the largest number of patients described to date involving two independent data sets. The conclusions based on our molecular analyses provide a basis for future preclinical studies using large cohorts of NSCLC models with differential expression of FGFR1 in order to validate the predictive value of this biomarker. Furthermore, our findings warrant the future investigation of the role of epigenetic regulatory mechanisms that modulate FGFR1 expression in NSCLC and other cancers. Patient selection based on FGFR1 protein expression may represent a more relevant approach compared to *FGFR1* amplification and should be considered in future clinical trials. Our findings encourage further clinical exploration of selective FGFR1 inhibitors as a targeted therapy concept in FGFR1-driven cancers.

Authors contributions (CRediT statements)

Olga Bogatyrova: Methodology, Software, Validation, Formal analysis, Investigation, Visualization, Data curation, Writing – original draft, Writing – review & editing. **Johanna S.M. Mattsson**: Methodology, Validation, Investigation, Visualization, Data curation, Writing – original draft, Writing – review & editing. **Edith M. Ross**: Methodology, Software, Validation, Investigation, Data curation, Writing – original draft, Writing – review & editing. **Michael P. Sanderson**: Conceptualization, Project administration, Writing – original draft, Writing – review & editing. **Max Backman**: Investigation, Data curation. **Johan Botling**: Resources, Project administration. **Hans Brunnström**: Resources, Data curation. **Pinja Kurppa**: Investigation. **Linnéa La Fleur**: Investigation. **Carina Strell**: Data curation, Writing – original draft. **Claudia Wilm**: Investigation, Writing – original draft. **Astrid Zimmermann**: Investigation, Writing – original draft. **Christina Esdar**: Conceptualization, Resources, Supervision, Project administration, Writing – original draft, Writing – review & editing. **Patrick Micke**: Conceptualization, Resources, Supervision, Project administration, Writing – original draft, Writing – review & editing

Financial support

Financial support for this study was provided by Merck KGaA, Darmstadt, Germany. This study was partly supported by The Swedish Cancer Society, The Lions Cancer Foundation Uppsala, Sweden, Selanders Foundation, and The Sjöberg Foundation, Sweden.

Conflict of interest statement

The authors declare the following financial interests/personal relationships which may be considered as potential competing interests: Astrid Zimmermann, Christina Esdar, Claudia Wilm, Edith M. Ross, Olga Bogatyrova and Michael P. Sanderson are employees and/or stockholders of Merck KGaA, Darmstadt, Germany. All other authors declare no conflicts of interest. Patrick Micke. On behalf of all co-authors.

Acknowledgements

We acknowledge Lars Björk (ContextVision) for assistance in the scanning of the FGFR1 FISH slides. We thank Anne-Kathrin Prokein and Patrick Steiner (both from Merck KGaA) for coordinating the *in vivo* pharmacology studies. We are grateful to Teresa Dolt, Eike Staub and Anja Victor (all from Merck KGaA) for their critical input and scientific insights. The results shown here are in whole or partly based upon data generated by TCGA Research Network: https://www.cancer.gov/tcga.

Appendix A. Supplementary data

Supplementary data to this article can be found online at https://doi.org/10.1016/j.ejca.2021.04.005.

References

[1] Janku F, Stewart DJ, Kurzrock R. Targeted therapy in non-small-cell lung cancer—is it becoming a reality? Nat Rev Clin Oncol 2010;7(7):401–14.
[2] Westphalen BC, Bokemeyer C, Buttner R, Frohling S, Gaidzik VI, Glimm H, et al. Conceptual framework for precision cancer medicine in Germany: consensus statement of the Deutsche Krebshilfe working group 'Molecular Diagnostics and Therapy. Eur J Canc 2020;135:1–7.
[3] Sasaki T, Rodig SJ, Chirieac LR, Janne PA. The biology and treatment of EML4-ALK non-small cell lung cancer. Eur J Canc 2010;46(10):1773–80.
[4] Meador CB, Micheel CM, Levy MA, Lovly CM, Horn L, Warner JL, et al. Beyond histology: translating tumor genotypes into clinically effective targeted therapies. Clin Canc Res 2014;20(9):2264–75.
[5] Baselga J. Targeting tyrosine kinases in cancer: the second wave. Science 2006;312(5777):1175–8.
[6] Devarakonda S, Morgensztern D, Govindan R. Genomic alterations in lung adenocarcinoma. Lancet Oncol 2015;16(7):e342–51.
[7] Preusser M, Berghoff AS, Koller R, Zielinski CC, Hainfellner JA, Liebmann-Reindl S, et al. Spectrum of gene mutations detected by next generation exome sequencing in brain metastases of lung adenocarcinoma. Eur J Canc 2015;51(13):1803–11.
[8] Lai WV, Lebas L, Barnes TA, Milia J, Ni A, Gautschi O, et al. Afatinib in patients with metastatic or recurrent HER2-mutant

lung cancers: a retrospective international multicentre study. Eur J Canc 2019;109:28–35.
[9] Jones RL, Ratain MJ, O'Dwyer PJ, Siu LL, Jassem J, Medioni J, et al. Phase II randomised discontinuation trial of brivanib in patients with advanced solid tumours. Eur J Canc 2019;120:132–9.
[10] Custodio A, Mendez M, Provencio M. Targeted therapies for advanced non-small-cell lung cancer: current status and future implications. Canc Treat Rev 2012;38(1):36–53.
[11] Drilon A, Oxnard GR, Tan DSW, Loong HHF, Johnson M, Gainor J, et al. Efficacy of selpercatinib in RET fusion-positive non-small-cell lung cancer. N Engl J Med 2020;383(9):813–24.
[12] Gainor JF, Lee DH, Curigliano G, Doebele RC, Kim D-W, Baik CS, et al. Clinical activity and tolerability of BLU-667, a highly potent and selective RET inhibitor, in patients (pts) with advanced RET-fusion+ non-small cell lung cancer (NSCLC). J Clin Oncol 2019;37(15_suppl):9008.
[13] Passiglia F, Malapelle U, Del Re M, Righi L, Pagni F, Furlan D, et al. KRAS inhibition in non-small cell lung cancer: past failures, new findings and upcoming challenges. Eur J Canc 2020;137:57–68.
[14] Canon J, Rex K, Saiki AY, Mohr C, Cooke K, Bagal D, et al. The clinical KRAS(G12C) inhibitor AMG 510 drives anti-tumour immunity. Nature 2019;575(7781):217–23.
[15] Wang Y, Ding X, Wang S, Moser CD, Shaleh HM, Mohamed EA, et al. Antitumor effect of FGFR inhibitors on a novel cholangiocarcinoma patient derived xenograft mouse model endogenously expressing an FGFR2-CCDC6 fusion protein. Canc Lett 2016;380(1):163–73.
[16] Turner N, Grose R. Fibroblast growth factor signalling: from development to cancer. Nat Rev Canc 2010;10(2):116–29.
[17] Facchinetti F, Hollebecque A, Bahleda R, Loriot Y, Olaussen KA, Massard C, et al. Facts and new hopes on selective FGFR inhibitors in solid tumors. Clin Canc Res 2020;26(4):764–74.
[18] Loriot Y, Necchi A, Park SH, Garcia-Donas J, Huddart R, Burgess E, et al. Erdafitinib in locally advanced or metastatic urothelial carcinoma. N Engl J Med 2019;381(4):338–48.
[19] Abou-Alfa GK, Sahai V, Hollebecque A, Vaccaro G, Melisi D, Al-Rajabi R, et al. Pemigatinib for previously treated, locally advanced or metastatic cholangiocarcinoma: a multicentre, open-label, phase 2 study. Lancet Oncol 2020;21(5):671–84.
[20] Weiss J, Sos ML, Seidel D, Peifer M, Zander T, Heuckmann JM, et al. Frequent and focal FGFR1 amplification associates with therapeutically tractable FGFR1 dependency in squamous cell lung cancer. Sci Transl Med 2010;2(62):62ra93.
[21] Turner N, Pearson A, Sharpe R, Lambros M, Geyer F, Lopez-Garcia MA, et al. FGFR1 amplification drives endocrine therapy resistance and is a therapeutic target in breast cancer. Canc Res 2010;70(5):2085–94.
[22] Aggarwal C, Redman MW, Lara Jr PN, Borghaei H, Hoffman P, Bradley JD, et al. SWOG S1400D (NCT02965378), a phase II study of the fibroblast growth factor receptor inhibitor AZD4547 in previously treated patients with fibroblast growth factor pathway-activated stage IV squamous cell lung cancer (Lung-MAP substudy). J Thorac Oncol 2019;14(10):1847–52.
[23] Chae YK, Hong F, Vaklavas C, Cheng HH, Hammerman P, Mitchell EP, et al. Phase II study of AZD4547 in patients with tumors harboring aberrations in the FGFR pathway: results from the NCI-MATCH trial (EAY131) subprotocol W. J Clin Oncol 2020;38(21):2407–17.
[24] Nogova L, Sequist LV, Perez Garcia JM, Andre F, Delord JP, Hidalgo M, et al. Evaluation of BGJ398, a fibroblast growth factor receptor 1-3 kinase inhibitor, in patients with advanced solid tumors harboring genetic alterations in fibroblast growth factor receptors: results of a global phase I, dose-escalation and dose-expansion study. J Clin Oncol 2017;35(2):157–65.
[25] Paik PK, Shen R, Berger MF, Ferry D, Soria JC, Mathewson A, et al. A phase Ib open-label multicenter study of AZD4547 in patients with advanced squamous cell lung cancers. Clin Canc Res 2017;23(18):5366–73.
[26] Mattsson JS, Bergman B, Grinberg M, Edlund K, Marincevic M, Jirstrom K, et al. Prognostic impact of COX-2 in non-small cell lung cancer: a comprehensive compartment-specific evaluation of tumor and stromal cell expression. Canc Lett 2015;356(2 Pt B):837–45.
[27] Botling J, Edlund K, Lohr M, Hellwig B, Holmberg L, Lambe M, et al. Biomarker discovery in non-small cell lung cancer: integrating gene expression profiling, meta-analysis, and tissue microarray validation. Clin Canc Res 2013;19(1):194–204.
[28] Micke P, Mattsson JS, Djureinovic D, Nodin B, Jirstrom K, Tran L, et al. The impact of the fourth edition of the WHO classification of lung tumours on histological classification of resected pulmonary NSCCs. J Thorac Oncol 2016;11(6):862–72.
[29] Tran L, Mattsson JS, Nodin B, Jonsson P, Planck M, Jirstrom K, et al. Various antibody clones of Napsin A, thyroid transcription factor 1, and p40 and comparisons with cytokeratin 5 and p63 in histopathologic Diagnostics of non-small cell lung carcinoma. Appl Immunohistochem Mol Morphol 2016;24(9):648–59.
[30] Miyashita N, Horie M, Mikami Y, Urushiyama H, Fukuda K, Miyakawa K, et al. ASCL1 promotes tumor progression through cell-autonomous signaling and immune modulation in a subset of lung adenocarcinoma. Canc Lett 2020;489:121–32.
[31] Mezheyeuski A, Bergsland CH, Backman M, Djureinovic D, Sjoblom T, Bruun J, et al. Multispectral imaging for quantitative and compartment-specific immune infiltrates reveals distinct immune profiles that classify lung cancer patients. J Pathol 2018;244(4):421–31.
[32] Schildhaus HU, Heukamp LC, Merkelbach-Bruse S, Riesner K, Schmitz K, Binot E, et al. Definition of a fluorescence in-situ hybridization score identifies high- and low-level FGFR1 amplification types in squamous cell lung cancer. Mod Pathol 2012;25(11):1473–80.
[33] Jabs V, Edlund K, Konig H, Grinberg M, Madjar K, Rahnenfuhrer J, et al. Integrative analysis of genome-wide gene copy number changes and gene expression in non-small cell lung cancer. PLoS One 2017;12(11):e0187246.
[34] Djureinovic D, Hallstrom BM, Horie M, Mattsson JSM, La Fleur L, Fagerberg L, et al. Profiling cancer testis antigens in non-small-cell lung cancer. JCI Insight 2016;1(10):e86837.
[35] Hellwig B, Hengstler JG, Schmidt M, Gehrmann MC, Schormann W, Rahnenfuhrer J. Comparison of scores for bimodality of gene expression distributions and genome-wide evaluation of the prognostic relevance of high-scoring genes. BMC Bioinf 2010;11:276.
[36] La Fleur L, Falk-Sorqvist E, Smeds P, Berglund A, Sundstrom M, Mattsson JS, et al. Mutation patterns in a population-based non-small cell lung cancer cohort and prognostic impact of concomitant mutations in KRAS and TP53 or STK11. Lung Canc 2019;130:50–8.
[37] Collado-Torres L, Nellore A, Jaffe AE. Recount workflow: accessing over 70,000 human RNA-seq samples with Bioconductor. F1000Res 2017;6:1558.
[38] Kahles A, Lehmann KV, Toussaint NC, Huser M, Stark SG, Sachsenberg T, et al. Comprehensive analysis of alternative splicing across tumors from 8,705 patients. Canc Cell 2018;34(2):211–224 e6.
[39] Thorsson V, Gibbs DL, Brown SD, Wolf D, Bortone DS, Ou Yang TH, et al. The immune landscape of cancer. Immunity 2018;48(4):812–830 e14.
[40] Therasse P, Arbuck SG, Eisenhauer EA, Wanders J, Kaplan RS, Rubinstein L, et al. New guidelines to evaluate the response to treatment in solid tumors. European Organization for Research and treatment of cancer, National cancer Institute of the United

States, National cancer Institute of Canada. J Natl Cancer Inst 2000;92(3):205–16.
[41] Hsu SD, Lin FM, Wu WY, Liang C, Huang WC, Chan WL, et al. miRTarBase: a database curates experimentally validated microRNA-target interactions. Nucleic Acids Res 2011;39(Database issue):D163–9.
[42] Esdar C, Iffland C, Zimmermann A, Lim A, Sanderson M, Blaukat A. Abstract 4853: M6123 is an ADCC-enhanced and selective monovalent antagonist of FGFR1 showing antitumor activity in preclinical lung cancer models. Canc Res 2019;79(13 Supplement):4853.
[43] Yu P, Knippel A, Onidi M, Paoletti A, Vigna E, Hellmann J, et al. A novel monovalent FGFR1 antagonist: preclinical safety profiles in rodents and non-human primates. Toxicol Appl Pharmacol 2020;406:115215.
[44] Zhang J, Zhang L, Su X, Li M, Xie L, Malchers F, et al. Translating the therapeutic potential of AZD4547 in FGFR1-amplified non-small cell lung cancer through the use of patient-derived tumor xenograft models. Clin Canc Res 2012;18(24):6658–67.
[45] Gudernova I, Vesela I, Balek L, Buchtova M, Dosedelova H, Kunova M, et al. Multikinase activity of fibroblast growth factor receptor (FGFR) inhibitors SU5402, PD173074, AZD1480, AZD4547 and BGJ398 compromises the use of small chemicals targeting FGFR catalytic activity for therapy of short-stature syndromes. Hum Mol Genet 2016;25(1):9–23.
[46] Wynes MW, Hinz TK, Gao D, Martini M, Marek LA, Ware KE, et al. FGFR1 mRNA and protein expression, not gene copy number, predict FGFR TKI sensitivity across all lung cancer histologies. Clin Canc Res 2014;20(12):3299–309.
[47] Kotani H, Ebi H, Kitai H, Nanjo S, Kita K, Huynh TG, et al. Co-active receptor tyrosine kinases mitigate the effect of FGFR inhibitors in FGFR1-amplified lung cancers with low FGFR1 protein expression. Oncogene 2016;35(27):3587–97.
[48] Weeden CE, Holik AZ, Young RJ, Ma SB, Garnier JM, Fox SB, et al. Cisplatin increases sensitivity to FGFR inhibition in patient-derived xenograft models of lung squamous cell carcinoma. Mol Canc Therapeut 2017;16(8):1610–22.
[49] Schuler M, Cho BC, Sayehli CM, Navarro A, Soo RA, Richly H, et al. Rogaratinib in patients with advanced cancers selected by FGFR mRNA expression: a phase 1 dose-escalation and dose-expansion study. Lancet Oncol 2019;20(10):1454–66.
[50] Kohler LH, Mireskandari M, Knosel T, Altendorf-Hofmann A, Kunze A, Schmidt A, et al. FGFR1 expression and gene copy numbers in human lung cancer. Virchows Arch 2012;461(1):49–57.
[51] Pros E, Lantuejoul S, Sanchez-Verde L, Castillo SD, Bonastre E, Suarez-Gauthier A, et al. Determining the profiles and parameters for gene amplification testing of growth factor receptors in lung cancer. Int J Canc 2013;133(4):898–907.
[52] Rooney C, Geh C, Williams V, Heuckmann JM, Menon R, Schneider P, et al. Characterization of FGFR1 locus in sqNSCLC reveals a broad and heterogeneous amplicon. PLoS One 2016;11(2):e0149628.
[53] Pekarsky Y, Balatti V, Croce CM. BCL2 and miR-15/16: from gene discovery to treatment. Cell Death Differ 2018;25(1):21–6.
[54] Andriani F, Majorini MT, Mano M, Landoni E, Miceli R, Facchinetti F, et al. MiR-16 regulates the pro-tumorigenic potential of lung fibroblasts through the inhibition of HGF production in an FGFR-1- and MEK1-dependent manner. J Hematol Oncol 2018;11(1):45.
[55] Lu T, Li Z, Yang Y, Ji W, Yu Y, Niu X, et al. The Hippo/YAP1 pathway interacts with FGFR1 signaling to maintain stemness in lung cancer. Canc Lett 2018;423:36–46.
[56] Chang J, Liu X, Wang S, Zhang Z, Wu Z, Zhang X, et al. Prognostic value of FGFR gene amplification in patients with different types of cancer: a systematic review and meta-analysis. PLoS One 2014;9(8):e105524.
[57] Le X, Negrao MV, Reuben A, Federico L, Diao L, McGrail D, et al. Characterization of the immune landscape of EGFR-mutant NSCLC identifies CD73/adenosine pathway as a potential therapeutic target. J Thorac Oncol 2021;16(4):583–600. https://doi.org/10.1016/j.jtho.2020.12.010.
[58] Song SG, Kim S, Koh J, Yim J, Han B, Kim YA, et al. Comparative analysis of the tumor immune-microenvironment of primary and brain metastases of non-small-cell lung cancer reveals organ-specific and EGFR mutation-dependent unique immune landscape. Cancer Immunol Immunother 2021. https://doi.org/10.1007/s00262-020-02840-0.
[59] Suda K, Mitsudomi T, Shintani Y, Okami J, Ito H, Ohtsuka T, et al. Clinical impacts of EGFR mutation status: analysis of 5780 surgically resected lung cancer cases. Ann Thorac Surg 2021;111(1):269–76.
[60] Biton J, Mansuet-Lupo A, Pecuchet N, Alifano M, Ouakrim H, Arrondeau J, et al. TP53, STK11, and EGFR mutations predict tumor immune profile and the response to anti-PD-1 in lung adenocarcinoma. Clin Canc Res 2018;24(22):5710–23.
[61] Koyama S, Akbay EA, Li YY, Aref AR, Skoulidis F, Herter-Sprie GS, et al. STK11/LKB1 deficiency promotes neutrophil recruitment and proinflammatory cytokine production to suppress T-cell activity in the lung tumor microenvironment. Canc Res 2016;76(5):999–1008.
[62] Luke JJ, Bao R, Sweis RF, Spranger S, Gajewski TF. WNT/beta-catenin pathway activation correlates with immune exclusion across human cancers. Clin Canc Res 2019;25(10):3074–83.
[63] Spranger S, Dai D, Horton B, Gajewski TF. Tumor-residing Batf3 dendritic cells are required for effector T cell trafficking and adoptive T cell therapy. Canc Cell 2017;31(5):711–723 e4.
[64] Dong ZY, Zhang JT, Liu SY, Su J, Zhang C, Xie Z, et al. EGFR mutation correlates with uninflamed phenotype and weak immunogenicity, causing impaired response to PD-1 blockade in non-small cell lung cancer. OncoImmunology 2017;6(11):e1356145.
[65] Sugiyama E, Togashi Y, Takeuchi Y, Shinya S, Tada Y, Kataoka K, et al. Blockade of EGFR improves responsiveness to PD-1 blockade in EGFR-mutated non-small cell lung cancer. Sci Immunol 2020;5(43).